Analysis of mica inclusions using LA-ICP-MS: 1 a new approach for sourcing raw material of ceramics

Benjamin Gehres, Guirec Querré

Analysis of mica inclusions using LA-ICP-MS: a new approach for sourcing raw material of ceramics

Dr. Benjamin GEHRES
Doctor - University of Rennes 2 (France)

UMR 6566 CReAAH
263, Avenue du général Leclerc
Campus de Beaulieu
Building 24-25
University of Rennes 1
CS74205
35042 Rennes Cedex – France

Email : benjamin.gehres@gmail.com

Dr. Guirec QUERRÉ
Research engineer - French Ministry of Culture and Communication

UMR 6566 CReAAH
263, Avenue du général Leclerc
Campus de Beaulieu
Building 24-25
University of Rennes 1
CS74205
35042 Rennes Cedex – France

Email : guirec.querre@univ-rennes1.fr

Abstract:

The analytical methods used for determining the origin of archaeological ceramics, such as petrography, X-ray powder diffraction, X-ray fluorescence spectrometry, attain their limits for differentiating bodies of similar composition, especially when they derive from the alteration of granitoid rocks. Our new approach is based on the chemical analysis of biotite inclusions in ceramic bodies using laser ablation-inductively coupled plasma-mass spectrometry, and enables us to identify the geological origin of the clay used. Spot analysis of the biotite inclusions contained in ceramics made from clay derived from the alteration of rocks can be linked to the original granitic massif. The thin section or rock analysis of biotite inclusions is relatively fast. The dosage of trace elements, such as lithium and vanadium establishes a filiation between the rocks and ceramics. Using this geochemical base, it is possible to establish a link between a granitic batholite and early ceramics and to propose a circumscribed production area. This article will focus on occupations located on islands from western France.

Keywords: LA-ICP-MS, Sourcing, Ceramic, Raw material, Biotite

1. Introduction

In archaeology, the study of the origin of objects and of the raw materials in which they were made provides invaluable information for tracking relationships between different human groups for a given region and period, as well as recording the evolution of procurement throughout time. This is particularly true for archaeological ceramics, for which typochronology, but also composition and fabrication techniques are provenance criteria. At the present time, the most frequently used analytical methods for determining ceramic raw material sources are mineralogical and petrographic analyses with polarized light microscopy, X-ray powder diffraction (XRD), elementary chemical analyses using several techniques: pXRF (Hunt and Speakman, 2015), INAA (Speakman *et al*., 2011), ICP-OES (Tsolakidou and Kilikoglou, 2004), ICP-MS (Kennett *et al*., 2004). Other methods can be used and a more comprehensive list of these and their applications can be found in the literature (Rice 2006; Quinn 2009; 2013). The development of spectrometric spot analysis methods over the past few years paves the way for new perspectives in archaeometry (Sourcing of fluviatile shell temper: Peacock *et al.* 2007; elementary analyses of ceramics: Kennett *et al.* 2004; Golitko and Terrel 2012; U/Pb dating of inclusions of detrital zircons: Tochilin *et al.* 2012; distinction between fossil inclusions and shell temper: Gehres *et al.* 2015; characterization of archaeological materials: Speakman *et al.* 2002 ; 2011).
We used the laser ablation-inductively coupled plasma-mass spectrometry (LA-ICP-MS) method to characterize mineral phases included in ceramic bodies in order to determine their origin. In archaeology, the study of ceramic bodies is particularly interesting for tracing where they were made, among other aspects. In this way, these objects can be used to better evaluate exchange networks.
Apart from some organic tempers (ground bone, plants), the inclusions contained in ceramic bodies are mineral and these grains are characteristic of a specific geological source. The mineralogical and petrographic composition of archaeological ceramics generally reflects the geology of the place where they were produced, as workshops and production zones are generally close to raw materials sources. There are cases where the minerals, or assemblages of minerals from ceramic bodies are sufficiently rare and original to find their origin and define a presumably very restricted or even once-off production zone (Peacock 1988; Martineau *et al.* 2007; Quinn and Day 2007; Ixer and Vince, 2009), or where is a contrast in the composition of the geological substratum and the mineralogical composition of the bodies (Boileau *et al.* 2009).
When we work on archaeological sites located on crystalline bedrock with granite-gneissic rocks, it is very difficult to determine the massif or the formation of the original crystalline rocks from the alteration clays used to made ceramics, as a whole complex of formations have identical or close mineralogical compositions. In the geological formations existing on Earth, ancient cratons are generally composed of granite-gneissic rocks: like for example the Canadian Shield or the Baltic Shield.
This is the case in the Massif Central and the Armorican Massif in France (Fig. 1). There are numerous granite-gneissic formations in these cratons with very similar mineralogical composition, mainly made up of essential minerals such as quartz, plagioclase, potassium feldspar, micas such as biotite, muscovite) and at times smaller quantities of amphiboles and secondary minerals such as zircon, opaque minerals, rutile.
In order to develop our methodology, we worked on archaeological ceramics discovered in occupation sites mainly located in the Armorican Massif (Fig. 1), dating from the Neolithic and protohistory, from the end of the 5th millennium to the 1st century before our era. We used the LA-ICP-MS technique on thin sections to chemically characterize the biotite inclusions in ceramics and different rocks from the Armorican Massif (Fig. 1), where weathered and decayed rocks are likely to have been used by

potters. Indeed, chemical variations in the composition of these minerals are known to be very susceptible to the physico-chemical conditions of different magmas (Wones and Eugster 1965; Czamanske and Wones 1973; Helz 1973; Speer 1984; Haslam, 1968).

2. Origins of the studied ceramics (Table 1 / Fig. 2)

In order to test our method, we chose to work on ceramic productions issued from insular sites. By working on islands, we have access to local, slightly diversified geological formations, creating more favourable conditions than on the mainland. The studied ceramics are from two archipelagos in the south of Brittany, one in the region of Carnac in Morbihan (Table 1, Fig. 2), the other in Finistère near Pont-Aven (Table 1, Fig. 2).

For the Houat-Hoedic archipelago, Belle-Île-en-Mer (Fig. 2), two ceramics from the Middle Neolithic I standing stone alignment (4700 - 4300 BCE) from Douet (Large *et al.* 2014) and one pottery from the salt fabrication workshop from the Second Iron Age (700 - 1st century BCE) from Port Blanc were used. A Bronze Age urn (850 - 700 BCE) with a granitic body from Belle-Île-en-Mer, completes the corpus from this archipelago. This pot was used as a container for a deposit of metallic objects (Audouard *et al.* 2010). One Hoedic granite sample, which is the only rock type on this island, is used as a reference sample to define the geological source. The petrographic analysis of these ceramics enabled us to observe inclusions characteristic of clays derived from the alteration of granite: grains of quartz, potassium feldspar and plagioclase, but also biotite and muscovite tablets. Rock fragments combining quartz, potassium feldspar and micas and presenting a grainy texture were also detected. Therefore, these potteries were made from granitic clay. However, it is not possible to determine whether they were made from the same clay, or clay from different sources.

For the Glénan Archipelago and Île aux Moutons (Fig. 2): three ceramics from the Middle Neolithic occupation II (4200 - 3800 BCE) from Île aux Moutons, three from the Second Iron Age settlement from Île aux Moutons (Daire and Hamon 2013) and two pottery from the Recent Neolithic settlement (3800 - 2800 BCE) from the Glénan Archipelago were used. These pots were made from clays with inclusions corresponding to the mineralogical composition of granitic rock. However, due to the marked similarity of the inclusions, it was not possible to differentiate the origin of these ceramics. Granite samples from Île aux Moutons and the Glénan Archipelago (one sample for each rock) were then used as local references and samples of granites from Beg Meil and Trégunc served as continental markers.

2.1. Geological context of the two archipelagos

Hoedic Island is mainly made up of granite with muscovite and biotite belonging to the family of granites from the south of the Armorican Massif formed during variscan tectogenesis (340 - 300 Ma) (Audren and Plaine 1986). The Belle-Île-en-Mer substratum is separated from the Houat-Hoedic complex by a NW-SE fault line, and is very different from the neighbouring islands. It is mainly made up of slightly metamorphic volcanic-sedimentary rocks: fine tuffs or porphyroids with a green schist facies (Table 2; Audren and Plaine 1986). Île aux Moutons and the Glénan Archipelago are the most northern islands off the southern coast of Brittany. Île aux Moutons is formed of a granitic base characterized by coarse feldspar grains (Delanoë and Pinot 1977). It is to highlight that this granite could be the same as the granite of Trégunc on the mainland, according to the 1/250000^{e} geological map (Thinon *et al.* 2009). The Glénan Archipelago is made up of at least two types of rock: a

porphyroid leucogranite carved by granitic rock with muscovite and granite with muscovite and biotite (Table 2; Béchennec *et al.* 1996).

3. Method

Spot chemical analyses were carried out with a quadrupole mass spectrometer with plasma source (Agilent Technologies, 7700 Series) coupled with a laser ablation system Nd:YAG of 213 nm (Cetac Technologies, LSX-213, G2). Laser ablation system conditions are the following: analysis time 180s, spot diameter: 20 μm, force ≈ 2.5 mJ/pulse, pulse width ≈ 5 ns, pulse frequency 20 Hz, ablation speed of 20 μm/s. Ablations are carried out on thin sections for archaeological pottery and directly on rock fragment references. After the drawing of the ablation layout, a quick ablation is made, with low energy and high speed, in order to homogenize the layout and remove possible pollution on the sample. 5 to 10 biotite tablets are analyzed per sample. The depth of the ablation is less than 30 μm and the inclusions can still be observed. The analysis of the average composition of each of the biotite inclusions with an average size generally ranging from 200 to 500 μm was obtained by laser scan on the whole inclusion.
The instrument is calibrated using international geological standards: DR-N, DT-N, UB-N (Govindaraju and Roelandts 1989) and MICA-Fe (Govindaraju and Roelandts 1988). Altogether, 46 elements were measured: Na, Mg, Al, Si, K, Ca, Ti, Mn, Fe, Li, Sc, V, Cr, Co, Ni, Cu, Zn, As, Rb, Sr, Y, Zr, Nb, Cd, Sb, Ba, La, Ce, Pr, Nd, Sm, Eu, Gd, Tb, Dy, Ho, Er, Tm, Yb, Lu, Hf, Ta, Tl, Pb, Th, U.

The analysis results from biotite inclusions (Tables 3 and 4) contained in rocks and ceramics reveal several elements enabling us to differentiate biotites depending on their origin. Indeed, the internal variation of the chemical composition within sources is low and allow to determine the origin of each rocks and ceramics. The major element have been converted into oxide forms (Na_2O, MgO, Al_2O_3, SiO_2, K_2O, CaO, TiO_2, MnO, and Fe2O3) and the REE have been chondrite-normalized (McDonough & Sun 1995).

4. Results and discussion

To identify the elements who allowed us to distinguish the different granites, the results of the different analysis of biotites from the granites from Île aux Moutons, the Glénan Archipelago and also from Beg Meil and Trégunc on the mainland, have been grouped using the principal component analysis (Fig. 3). Thus, we can observe that the granite from Île aux Moutons and Trégunc are not differentiable, but the granites from the Glénan Archipelago and from Beg Meil are clearly distinguishable from the other rocks (Fig. 3). A cluster analysis of the measured elements allow us to determine the main elements that can distinguish the different sources: Li, V, Zn, Sr (Fig. 4). Two elements are particularly relevant; lithium - known for fixing mainly in mica tablets (Siroonian *et al.* 1959; Kuts and Mishchenko 1963) - and vanadium.

4.1. Houat-Hoedic-Belle-Île-en-Mer complex (Fig. 2)

The analyses of the biotite inclusions in four ceramics from the sites of Hoedic and one from Belle-Île-en-Mer show dispersed composition (Fig. 5; Table 3). In the V versus Li diagram, the representative points of the analyses are placed along two lines corresponding to very different Li/V ratios.

The first group of analyses presents a very high Li/V ratio with biotites with low vanadium contents; these analyses correspond to the pottery from Belle-Île-en-Mer. The second group of analysis presents a much lower Li/V ratio with low lithium values. These analyses correspond to the pottery from Hoedic. These variations in Li concentration in biotites are generally linked to the intensity of hydrothermal granite alterations (Konings *et al.* 1988). Therefore, this technique enables us to differentiate compositions of trace elements in two types of ceramic productions with similar petrographic characteristics. Moreover, the two composition groups probably correspond to two different geological origins (Fig. 5). No granitic rocks outcrop on Belle-Île-en-Mer, where the geological formations are largely dominated by green schists (Audren and Plaine 1986). Thus the analyzed urn can only correspond to an imported vessel. According to biotite analyses by LA-ICP-MS, the hypothesis of the importation of this urn to Belle-Île-en-mer from Hoedic or Houat must be rejected. Therefore, the urn was made on the mainland from clay derived from the alteration of granitic rock. However, the production zone has yet to be more accurately defined.

Biotite analyzes of the Hoedic granite follow the same line as those of the biotites included in the ceramics discovered on this same island (Fig. 5). Furthermore, all the analyzed biotites in a single sample have the same composition range, who is broader for the rock than for ceramics, but always with the same Li/V ratio for both of them. The ceramics were thus probably made from clay derived from the alteration of local rock. Consequently, this is a local non-imported production.

4.2. Glénan Archipelago - Île aux Moutons complex (Fig. 2)

Eight ceramics discovered on these different islands were selected for chemical LA-ICP-MS spot analyses on the basis of the presence of biotite inclusions in ceramic raw materials from the Île aux moutons and the Glénan Archipelago sites. Furthermore, by comparing the analyses of biotites from local and continental granites, it should be possible to find the rocks that formed these clays by alteration.

The results show that biotite compositions of ceramic bodies are not homogeneous, but develop around regression lines (Fig. 6; Table 4).

Biotite analyses are recorded in the same V versus Li diagram as for the previous case. The points are distributed in composition groups defining the lines with different V/Li ratios.

The Li/V ratio is between 1.84 and 7.34 for biotites from ceramics for which the raw material comes from Île aux Moutons, whereas the Li/V ratio of biotites from pottery made with clays derived from the alteration of the Beg Meil granite ranges between 0.06 and 2.12. Lastly, the Li/V ratio of biotites from the Glénan Archipelago granite is between 73.51 and 242.22.

Three sets of points can be differentiated (Fig. 6). Two are made up of ceramic and granite biotite and the other only of granite biotite. The first group corresponds to biotite inclusions with little Li, between 0 and 300 ppm and very dispersed V values, ranging from several tens of ppm to nearly 800 ppm. These inclusions correspond to Neolithic ceramics from Île aux Moutons and the Glénan Archipelago, as well as vessels from the Second Iron Age from Île aux Moutons. The Beg Meil continental granite, located 10 km to the north of the archaeological sites is also in this group. Indeed, biotites from ceramics and rock sample have the same Li/V range ratio. However, it is possible to observe that the Li concentrations is higher in the rock, because of the alteration of the biotite crystals.

A second set groups is composed by Neolithic ceramics discovered on the Glénan Archipelago and Iron Age ceramics on the Île aux Moutons, as well as to the Île aux Moutons granite and the continental granite from B, situated 12 km northwest of the archaeological sites. This observation

confirm that the granites from Trégunc and Île aux Moutons are the same. The last set only contains granite biotites from the Glénan Archipelago.
Therefore, the LA-ICP-MS analyses confirm the utilization of two clay sources on these islands. By extension, it is now possible to deduce the origin of the other ceramics discovered on these islands. In this way, we observe that exchanges with the mainland took place during the Neolithic, but also that pottery was produced on Île aux Moutons and exported into the Glénan Archipelago. During the Second Iron Age, this production no longer exists and all the vases are imported from the continent to Île aux Moutons. Lastly, we note that no vessels appear to have been made from the clays derived from granite alteration in the Glénan Archipelago during these periods.
These conclusions raise questions as to the type of occupations on these islands. They may have consisted of seasonal occupations by mainland populations, during the harvesting of certain marine products.

Conclusions

The chemical spot analysis of mineral inclusions in archaeological ceramic bodies using LA-ICP-MS opens new prospects in terms of sourcing. The comparison of the analyses of biotite inclusions in ceramics and the granitic rocks liable to have supplied pottery clays by alteration, using Armorican samples, validates the method. The possibility of simultaneously analyzing very light elements like lithium with this technique, which is generally difficult to measure, and heavier elements on very small volumes of the size of an infra millimetric inclusion, is particularly potent. This is not the case with commonly used techniques, such as Castaing electron microprobe (Froh 2004), ICP-AES (Bruno *et al.* 2000) or PIXE, for example (Roumié *et al.* 2006).
This is a rapid method that requires little sample preparation: ablation is carried out directly on ceramics, rocks or uncovered thin sections, unlike methods such as ICP-AES, which necessitates Frantz magnetic separation (Konings *et al.* 1988) and which can do spot analyses, in contrast to PIGE (Calligaro *et al.* 2000, Bugoi *et al.* 2008).
Results are obtained rapidly; analysis time is 180s for measuring 46 elements. The measurement of limited quantities of elements improves the analysis results and leads to the analysis of more biotite inclusions.

In those examples, we didn't find biotites with more than one geochemical composition in a single sherd. This can be explain by the utilization of non-mixed clays, coming from a unique mother rock. However, it can be possible that potters used mixed clays from alluvial deposits or have added crushed rocks. In this case, it is possible to obtain several geochemical composition and different Li/V ratios that represent each origins (Gehres, 2016).

The application of this new method to archaeological ceramics could be extended to minerals other than biotite from granitic rocks when this material is not sufficiently abundant in ceramic bodies and source rocks. Indeed, our work have been extended to the gabbroic clay with the analyses of amphibole grains and ultrabasic clay with the studies of opaque mineral (Gehres, 2016; Gehres and Querré, under press).

Acknowledgments

The authors would like to thank J.-C Le Bannier for his technical assistance, M.-Y. Daire, G. Hamon, J.-M Large, G. Musch, for the lending of the archaeological collections.

Reference list

AUDOUARD, L., BARRACAND, G., TARAUD, T., MUSCH, G. (2010). Belle-Île-en-Mer du Mésolithique à l'âge du Bronze : Emergence d'une nouvelle dynamique de recherche. *Bulletin de l'Association Manche Atlantique pour la Recherche Archéologique dans les Îles*, 23, 17-36.

AUDREN, C., PLAINE, J. (1986). *Notice explicative, Carte géol. France (1/50 000), feuille Belle-Île-en-Mer (447-477).* Orléans: Bureau de Recherches Géologiques et Minières.

BÉCHENNEC, F., GUENNOC, P., GUERROT, C., LEBRET, P., THIÉBLEMONT, D., with the collaboration of CARN, A., DELANOË, Y., GIOT, P.-R., HALLÉGOUËT, B., LE MEUR, S., MONNIER, J.-L., MORZADEC, H. (1996). Notice explicative, Carte géologique de France (1/50000), feuille Concarneau (382), Orléans: Bureau de Recherches Géologiques et Minières.

BOILEAU, M.-C., D'AGATA, A.L., WHITLEY, J. (2009). Pottery technology & regional exchange in Early Iron Age Crete. In: QUINN P.S. (Ed.), *Interpreting Silent Artefacts, Petrographic Approaches to Archaeological Ceramics* (pp. 157-172). Oxford: Archaeopress.

BRUNO, P., CASELLI, M., CURRI, M.L., GENGA, A., STRICCOLI, R., TRAINI, A. (2004). Chemical characterisation of ancient pottery from south of Italy by inductively coupled plasma atomic emission spectroscopy (ICP-AES), statistical multivariate analysis of data. *Anal. Chim. Acta*, 410, 193-202.

BUGOI, R., COJOCARU, V., CONSTANTINESCU, B., CALLIGARO, T., PICHON, L., RÖHRS, S., SALOMON, J. (2008). Compositional studies on Transylvanian gold nuggets: advantages and limitations of PIXE–PIGE analysis. *Nucl. Inst. Methods Phys. Res. B* 266, 2316-2319.

CALLIGARO, T., DRAN, J.-C., POIROT, J.-P., QUERRÉ, G., SALOMON, J., ZWAAN, J.-C. (2000). PIXE/PIGE characterisation of emeralds using an external microbeam. *Nucl. Inst. Methods Phys. Res. B* 161-163, 769-774.

CZAMANSKE, G.K., WONES, D.R. (1973). Oxidation during magmatic differentiation, Finnmarka complex, Oslo Ara Norway--ll. Mafic silicates. *Journal of Petrology*, 14, 349-380.

DAIRE, M.-Y., HAMON, G. (2013). *L'île aux Moutons (Fouesnant, Finistère) : un établissement gaulois dans son contexte atlantique*. Saint-Malo: Dossiers du Centre Régional d'Archéologie d'Alet.

DELANOË, Y., PINOT, J.-P. (1977). Littoraux et vallées holocènes submergés en Baie de Concarneau (Bretagne méridionale). *Bulletin de l'Association française pour l'Étude du Quaternaire*, 3, 27-38.

FROH, J., 2004 - Archaeological ceramics studied by scanning electron microscopy. *Hyperfine Interact.* 154(1), 159-176.

GEHRES B. (2016) - *Connaissances des sociétés insulaires armoricaines par l'étude archéométrique du mobilier céramique. Les réseaux d'échanges îles-continent : évolution du Néolithique à la période gallo-romaine,* Ph.D thesis, University of Rennes 2, 478.

GEHRES B., QUERRÉ G., La signature chimique des inclusions minérales comme traceur de l'origine des céramques : l'apport des analyses par LA-ICP-MS, In: BURNEZ-LANOTTE L. (Ed), *Matières à*

Penser: Raw materials acquisition and processing in Early Neolithic pottery productions, Proceedings of the Workshop of Namur (Belgium), 29 and 30 May 2015, Séances de la Société préhistorique française, 11, 2017, 177-197.

GEHRES B., QUERRÉ G., SAVARY X. with the collaboration of LE FORT A. (2015). Caractérisation des céramiques à bioclastes de la Protohistoire dans l'Ouest de la France. In: C. MOUGNE, M.-Y. DAIRE (Ed.), *L'Homme ses ressources et son environnement à l'âge du Fer dans le Nord-Ouest de la France, Actes du Séminaire Archéologique de l'Ouest* (105-119). Rennes: Mémoire de Geoscience Rennes, Hors-série n°9.

GOLITKO, M., TERREL, J. (2012). Mapping prehistoric social fields on the Sepik coast of Papua New Guinea: ceramic compositional analysis using laser ablation-inductively coupled plasma-mass spectrometry. *J. Archaeol. Sci.*, 39, 3568-3580.

GOVINDARAJU, K., ROELANDTS, I. (1988). *Geostand. Newslet.* 12, 119-201.

GOVINDARAJU, K., ROELANDTS, I. (1989). *Geostand. Newslet.* 13, 5-67.

HASLAM, H.W. (1968). The crystallization of intermediate and acid magmas at Ben Nevis, Scotland. *J. Petrol.* 9, 84-104.

HELZ, R.T. (1973). Phase relation of basalts in their melting range at P_{HO2} = 5 kb as a function of oxygen fugacity-1 Mafic phases. *J. Petrol.* 14, 429-502.

HUNT, M.W., SPEAKMAN, R.J. (2015). Portable XRF analysis of archaeological sediments and ceramics. *J. Archaeol. Sci.*, 53, 626-638.

IXER R., VINCE A.L. (2009). The provenance potential of igneous glacial erratics in Anglo-Saxon ceramics from Northern England. In: P. QUINN (Ed.), *Interpreting Silent Artefacts. Petrographic Approaches to Archaeological Ceramics*, Archaeopress, Oxford, 11-24.

KENNETT, D.J., ANDERSON, A.J., CRUZ, M.J., CLARK, G.R., SUMMERHAYES, G.R. (2004). Geochemical characterization of Lapita pottery via Inductively Coupled Plasma–mass Spectrometry (ICP–MS). *Archaeometry*, 46(1), 35-46.

KONINGS, R.J.M., BOLAND, J.N., VRIEND, S.P., JANSEN, J.B.H. (1988). Chemistry of biotites and muscovites in the Abas granite, northern Portugal. *Am. Mineral.*, 73, 754-765.

KUTS, V.P., MISHCHENKO, V.S. (1963). Distribution of lithium, rubidium, and some of the minerals that contain them in the Kamennyye Mogily and Yekaterninovka granites (Azov region). *Geochemistry*, 12, 1175-1192.

LARGE, J.-M., AUDOUARD, L., BRAGUIER, S., CARRION, Y., DELALANDE, C., DELOZE, V., DONNART, K., GEHRES, B., HAMON, G., JOLY, C., MARCOUX, N., MENS, E., QUERRÉ, G., VISSET, L. (2014). *La file de pierres dressées du Douet, Hoedic (Morbihan),* Jouve: Melvan.

MARTINEAU, R., WALTER-SIMONNET, A.-V., GROBÉTY, B. and BUATIER, M. (2007). Clay resources and technical choices for neolithic pottery (Chalain, Jura, France): chemical, mineralogical and grain-size analyses. *Archaeometry*, 49(1), 23-52.

McDONOUGH, W.F., SUN, S.-S. (1995). The composition of the Earth. *Chem. Geol.*, 120, 223-253.

PEACOCK, D. (1988). The gabbroic pottery of Cornwall. *Antiquity*, 62, 302 - 304.

PEACOCK, E., NEFF, H., RAFFERTY, J., MEAKER, T. (2007). Using laser ablation-inductively coupled plasma-mass spectrometry to source shell in shell-tempered pottery: a pilot study from north Mississippi. *Southeast. Archaeol.*, 42(1), 67-102.

QUINN, P. S., DAY, P. M. (2007). Calcareous microfossils in Bronze Age aegean ceramics: illuminating technology and provenance. *Archaeometry*, 49(4), 775-793.

QUINN, P. S. (2009). *Interpreting silent artefacts, petrographic approaches to archaeological ceramics*. Oxford: Archaeopress.

QUINN, P. S. (2013). *Ceramic petrography: the interpretation of archaeological pottery and related artefacts in thin section.* Oxford: Archaeopress.

RICE, P. (2006). *Pottery analysis, a sourcebook.* University of Chicago Press.

ROUMIÉ, M., REYNOLDS, P., ATALLAH, C., BAKRAJI, E., ZAHRAMAN, K., NSOULI, B. (2006). Provenance study of excavated pottery from Beirut using PIXE cluster analysis. *Ion Beam Analysis, Nucl. Instrum. Methods Phys. Res., Sect. B* 249(1-2), 612-615.

SIROONIAN, H.A., SHAW, D.M., JONES, R.E. (1959). Lithium geochemistry and the source of the spodumene pegmatites of the Pressac-Lamotte-Lacorne region of western Quebec. *The Canadian Mineralogist*, 6, 320-338.

SPEAKMAN, R.J., LITTLE N.C., CREEL D., RILLER M.R., IÑAÑEZ J.G. (2011). Sourcing ceramics with portable XRF spectrometers? A comparison with INAA using Mimbres pottery from the American Southwest. *Anal. Bioanal. Chem.* 374 (3), 566-572.

SPEAKMAN, R.J., NEFF, H., GLASCOCK, M.D. and HIGGINS, B.J. (2002). Characterization of archaeological materials by laser ablation-inductively coupled plasma-mass spectrometry. *American Chemical Society*, 48-63.

SPEER, J.A. (1984). Micas in igneous rocks. In: S.W. BAILEY (Ed.), *Micas* (pp. 299-356). Mineralogical Society of America.

THINON, I., MENIER, D., GUENNOC, P., PROUST, J.-N. (2009). *Carte géologique de la France à 1/250 000e de la marge continentale : Lorient, Bretagne Sud.* BRGM – CNRS.

TOCHILIN, C., DICKINSON, W., FELGATE, M., PECHA, M., SHEPPARD, P., DAMON, F., BICKLER, S., GEHRELS, G. (2012). Sourcing temper sands in ancient ceramics with U-Pb ages of detrital zircons: a southwest Pacific test case. *J. Archaeol.. Sci.* 39, 2583-2591.

TSOLAKIDOU A., KILIKOGLOU V. (2004). Comparative analysis of ancient ceramics by neutron activation analysis, inductively coupled plasma–optical-emission spectrometry, inductively coupled plasma–mass spectrometry, and X-ray fluorescence. *Archaeometry*, 46, 35-46.

WONES, D.R., EUGSTER, H.P. (1965). Stability of biotite: experiment, theory and application. *Am. Min.* 50, 1228-1273.

Captions

Fig.1 Simplified geological map of the Armorican massif

Fig.2 Case study areas mentioned in the text: (1) The islands of Houat, Hoedic and Belle-Île-en-Mer – (2) The Glénan Archipelago and the Île aux Moutons

Fig.3 Results of the Principal Component Analysis of the dataset (44 elements). The percentage of the total variance that is explained by the two principal components is 26.3 % and 17.5 %, respectively. The biotites from the five different granites analysed in the article are represented. The ellipses represent the 95% confidence ellipses.

- Biotite tablets from the granite of Beg Meil
- Biotite tablets from the granite of Île aux Moutons
- Biotite tablets from the granite of Glénan Archipelago
- Biotite tablets from the granite of Trégunc
- Biotite tablets from the granite of Hoedic

Fig.4 Hierarchical cluster analysis of the dataset with the Ward's method: Dendrogram displaying rescaled distance among the different element of the biotites from the five granites analysed.

Fig.5 Scatterplot of the concentrations obtained by LA-ICP-MS of Li and V (in ppm) of the analyzed biotites. Each point corresponds to an analyzed inclusion. The ellipses represent the 95% confidence ellipses.

- Biotite tablets from the granite of the Hoedic island.
- Biotite tablets from the ceramic (Douet 23) of the Middle Neolithic II site of Douet (Hoedic island)
- Biotite tablets from the ceramic (Douet 32) of the Middle Neolithic II site of Douet (Hoedic island)
- Biotite tablets from the ceramic of the Second Iron Age site of Port-Blanc (Hoedic island)
- Biotite tablets from the Bronze Age urn (Belle-Île-en-Mer).

Fig.6 Scatterplot of the concentrations obtained by LA-ICP-MS of Li and V (in ppm) of the analyzed biotites. Each point corresponds to an analyzed inclusion.

- Biotite tablets from the granite of Beg Meil
- Biotite tablets from the granite of Île aux Moutons
- Biotite tablets from the granite of Glénan Archipelago
- Biotite tablets from the granite of Trégunc
- Biotite tablets from the ceramic (Île aux Moutons Neo 4) of the Middle Neolithic II site of Île aux Moutons
- Biotite tablets from the ceramic (Île aux Moutons Neo 3) of the Middle Neolithic II site of Île aux Moutons
- Biotite tablets from the ceramic (Île aux Moutons Neo 9) of the Middle Neolithic II site of Île aux Moutons
- Biotite tablets from the ceramic (Saint Nicolas 3) of the Recent Neolithic site of Saint Nicolas (Glénan Archipelago)
- Biotite tablets from the ceramic (Saint Nicolas 10) of the Recent Neolithic site of Saint Nicolas (Glénan Archipelago)
- Biotite tablets from the ceramic (Île aux Moutons Iron Age 2) of the Second Iron Age site of Île aux Moutons
- Biotite tablets from the ceramic (Île aux Moutons Iron Age 4) of the Second Iron Age site of Île aux Moutons
- Biotite tablets from the ceramic (Île aux Moutons Iron Age 17) of the Second Iron Age site of Île aux Moutons

Table 1 Descriptions of the geographic origin of the archaeological sites and their occupation periods and location of the different granites mentioned

Table 2 Geological description of the mentioned insular complexes

Table 3 Average chemical composition and standard deviation of biotite in potteries and granite from Hoedic and Belle-Île-en-Mer

Table 4 Average chemical composition and standard deviation of biotite in potteries and granites from the Glénan

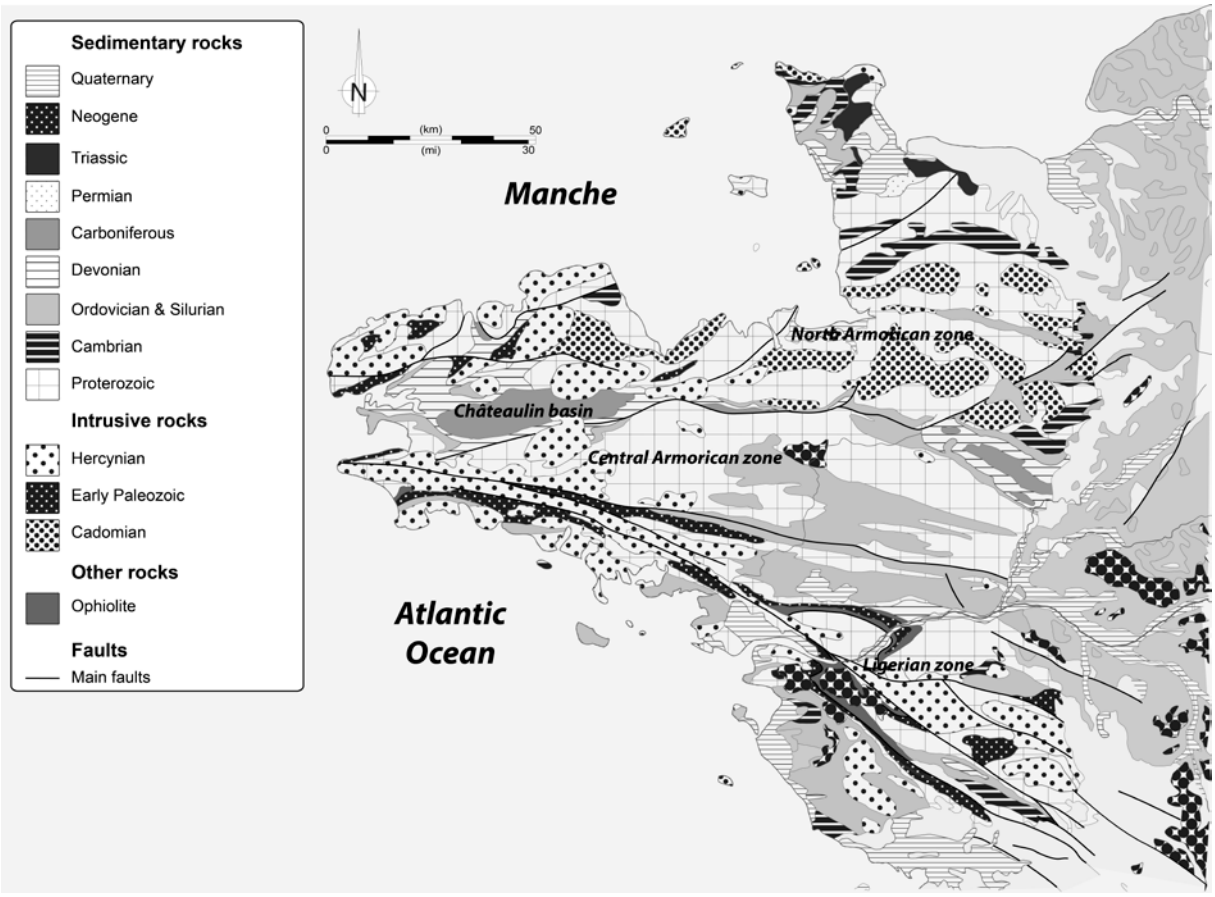

Fig.1 Simplified geological map of the Armorican massif

507
508 **Fig.2** Case study areas mentioned in the text: (1) The islands of Houat, Hoedic and Belle-Île-en-Mer – (2) The
509 Glénan Archipelago and the Île aux Moutons
510

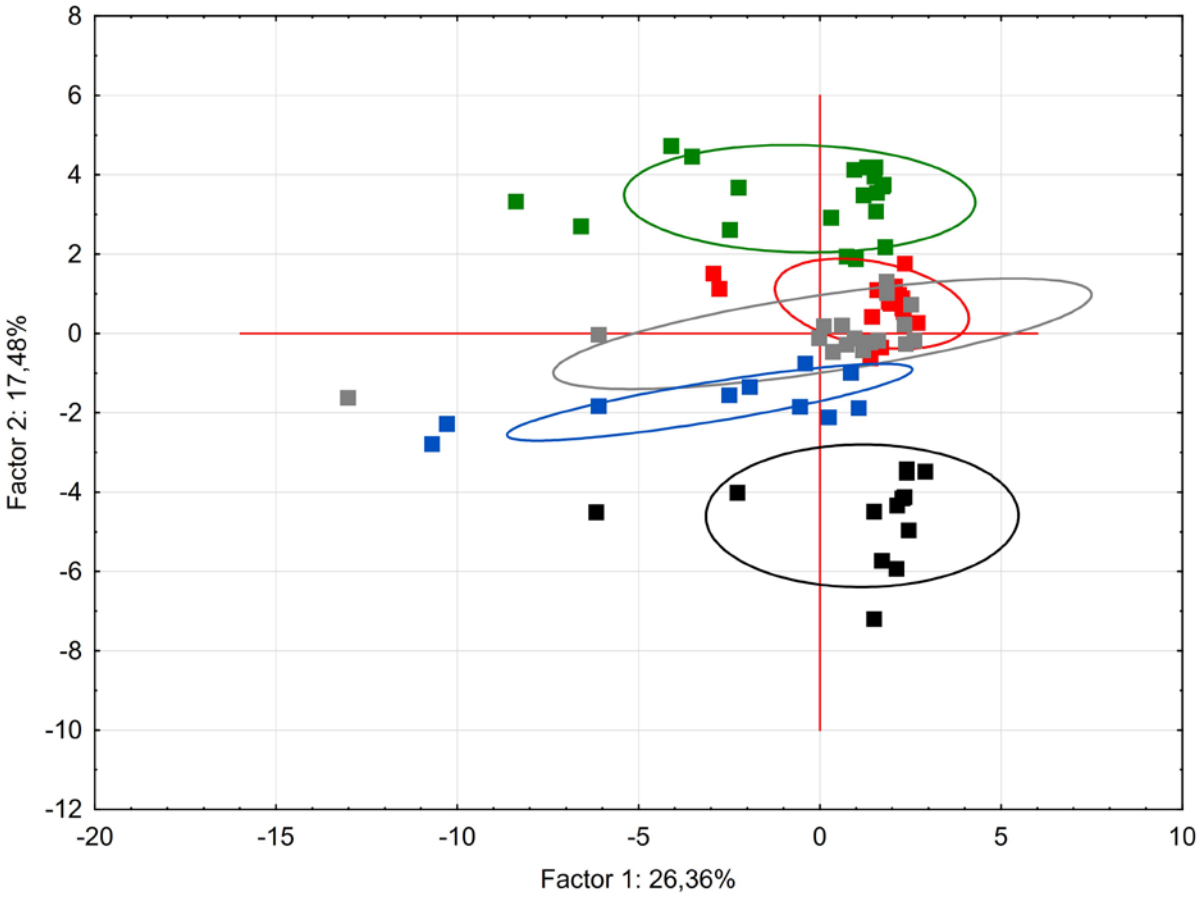

Fig.3 Results of the Principal Component Analysis of the dataset (44 elements). The percentage of the total variance that is explained by the two principal components is 26.3 % and 17.5 %, respectively. The biotites from the five different granites analysed in the article are represented. The ellipses represent the 95% confidence ellipses. Each point corresponds to an analysed inclusion from mother rocks.

- Biotite tablets from the granite of Beg Meil
- Biotite tablets from the granite of Île aux Moutons
- Biotite tablets from the granite of Glénan Archipelago
- Biotite tablets from the granite of Trégunc
- Biotite tablets from the granite of Hoedic

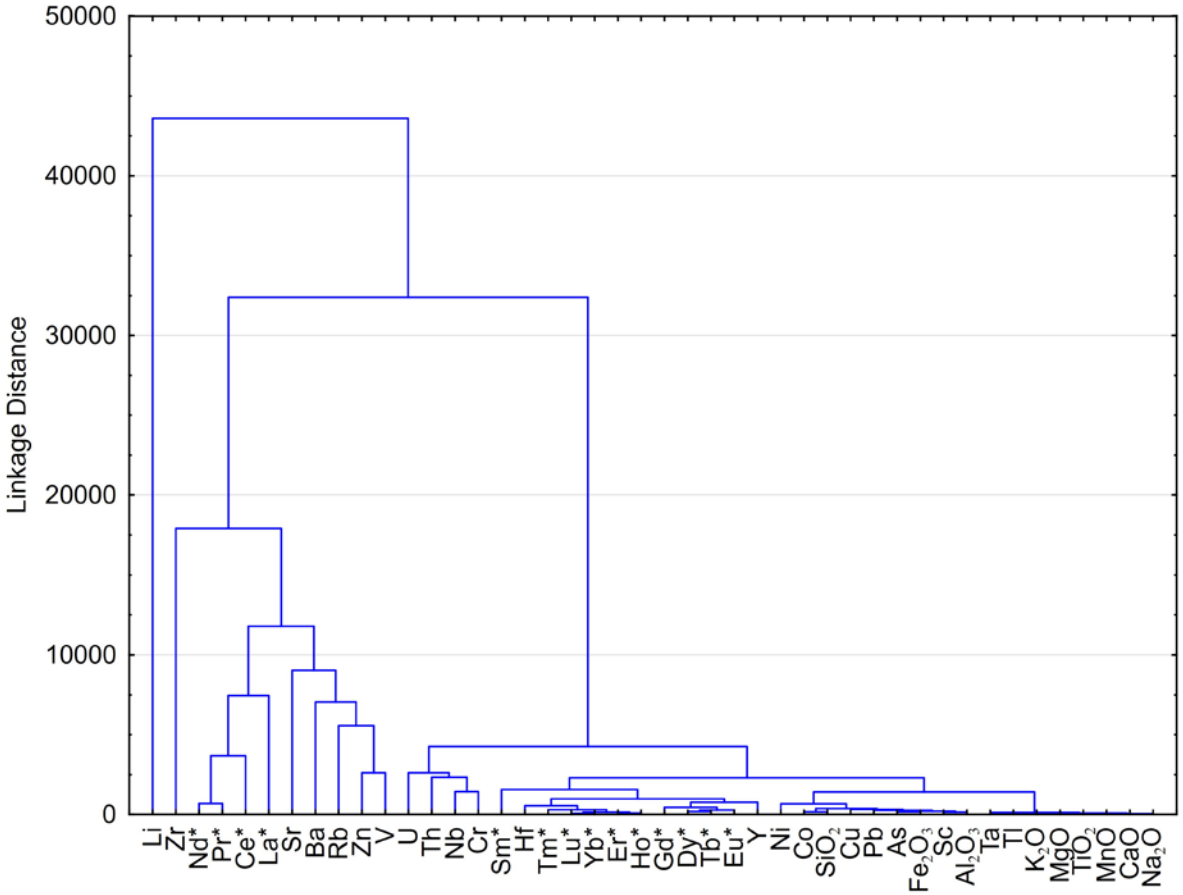

Fig.4 Hierarchical cluster analysis of the dataset with the Ward's method: Dendrogram displaying rescaled distance among the different element of the biotites from the five granites analyzed.

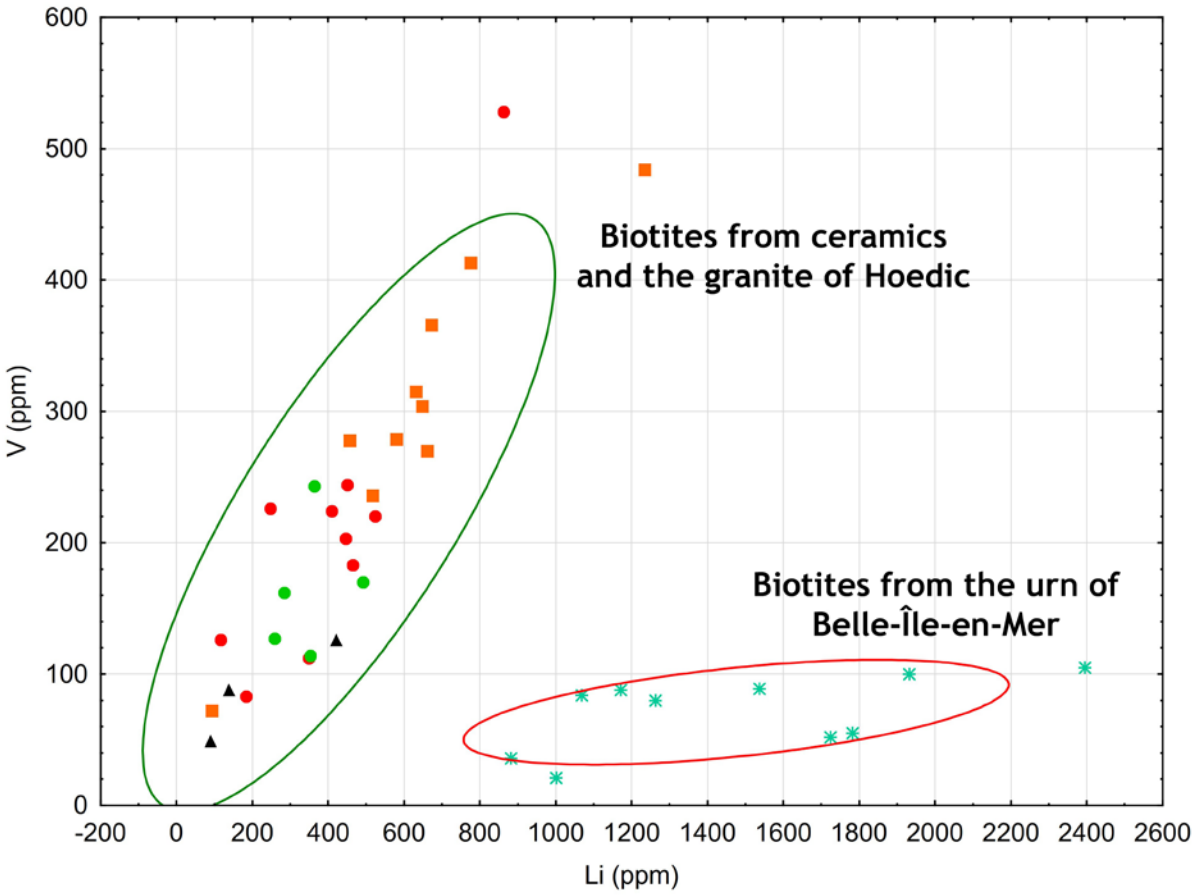

Fig.5 Scatterplot of the concentrations obtained by LA-ICP-MS of Li and V (in ppm) of the analyzed biotites. Each point corresponds to an analyzed inclusion. The ellipses represent the 95% confidence ellipses.

■ Biotite tablets from the granite of the Hoedic island.
● Biotite tablets from the ceramic (Douet 23) of the Middle Neolithic II site of Douet (Hoedic island)
● Biotite tablets from the ceramic (Douet 32) of the Middle Neolithic II site of Douet (Hoedic island)
▲ Biotite tablets from the ceramic of the Second Iron Age site of Port-Blanc (Hoedic island)
✱ Biotite tablets from the Bronze Age urn (Belle-Île-en-Mer).

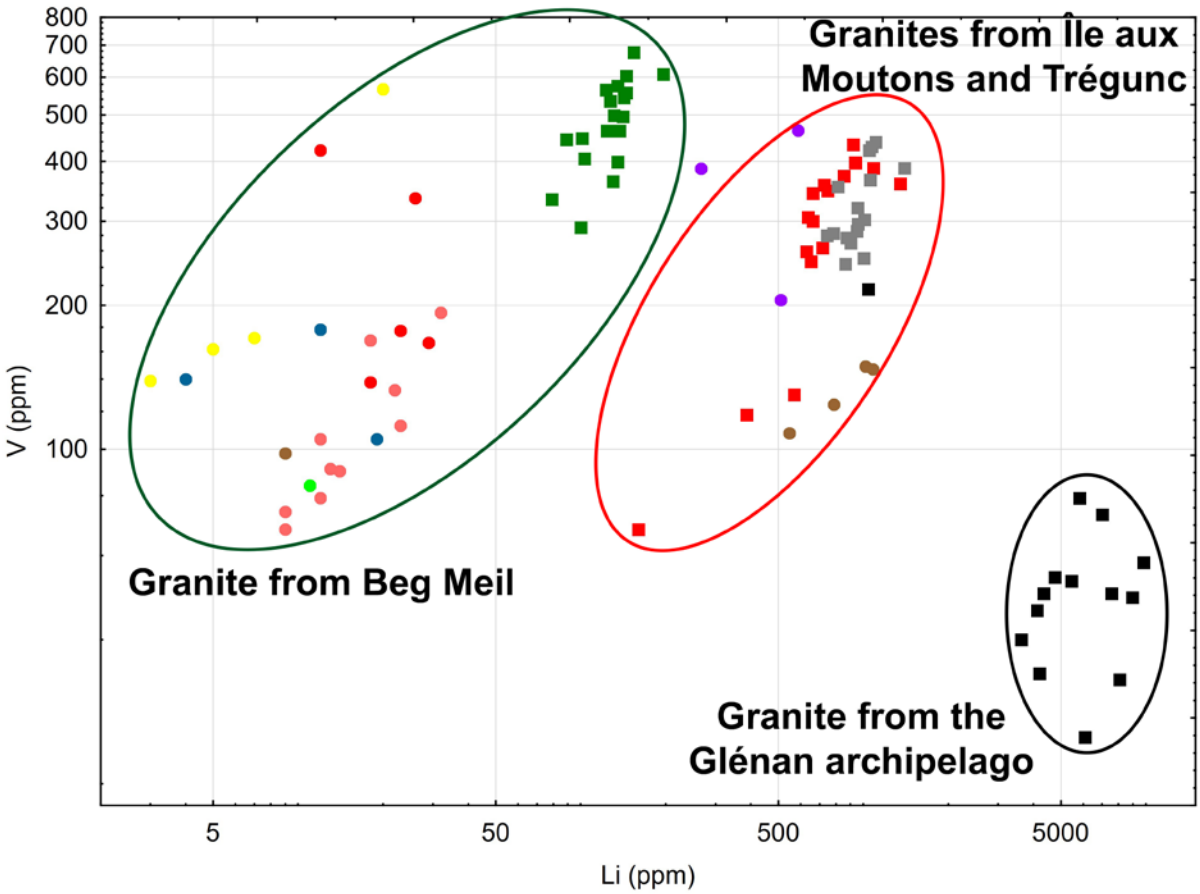

Fig.6 Scatterplot of the concentrations obtained by LA-ICP-MS of Li and V (in ppm) of the analyzed biotites. Each point corresponds to an analyzed inclusion.

- Biotite tablets from the granite of Beg Meil
- Biotite tablets from the granite of Île aux Moutons
- Biotite tablets from the granite of Glénan Archipelago
- Biotite tablets from the granite of Trégunc
- Biotite tablets from the ceramic (Île aux Moutons Neo 4) of the Middle Neolithic II site of Île aux Moutons
- Biotite tablets from the ceramic (Île aux Moutons Neo 3) of the Middle Neolithic II site of Île aux Moutons
- Biotite tablets from the ceramic (Île aux Moutons Neo 9) of the Middle Neolithic II site of Île aux Moutons
- Biotite tablets from the ceramic (Saint Nicolas 3) of the Recent Neolithic site of Saint Nicolas (Glénan Archipelago)
- Biotite tablets from the ceramic (Saint Nicolas 10) of the Recent Neolithic site of Saint Nicolas (Glénan Archipelago)
- Biotite tablets from the ceramic (Île aux Moutons Iron Age 2) of the Second Iron Age site of Île aux Moutons
- Biotite tablets from the ceramic (Île aux Moutons Iron Age 4) of the Second Iron Age site of Île aux Moutons
- Biotite tablets from the ceramic (Île aux Moutons Iron Age 17) of the Second Iron Age site of Île aux Moutons

		Island	Ceramic / Rock	Site	Period
Morbihan	**Houat-Hoedic Archipelago and Belle-Île-en-Mer**	*Hoedic*	C	Le Douet	Middle Neolithic II
			C	Port-Blanc	Second Iron Age
			R	Hoedic Granite as a standard	
		Belle-Île-en-Mer	C	Bordustard	Late Bronze Age III
Finistère	**Glénan Archipelago, Île aux Moutons**	*Île aux Moutons*	C	Île aux Moutons	Middle Neolithic II
			C	Île aux Moutons	Second Iron Age
			R	Granite from Île aux Moutons as a standard	
		Glénan Archipelago	C	Saint-Nicolas des Glénan	Recent Neolithic
			R	Glénan granite as a standard	
	Continent		R	Granite from Beg Meil as a standard	
			R	Granite de Trégunc as a standard	

Table 1 Descriptions of the geographic origin of the archaeological sites and their occupation periods and location of the different granites mentioned

	Island	Geology
Houat-Hoedic Archipelago and Belle-Île-en-Mer	*Houat-Hoedic*	Granite with muscovite and biotite
	Belle-Île en mer	Tuffs / porphyroid green schist facies
Glénan Archipelago, Île aux Moutons	*Île aux Moutons*	Porphyroid granite
	Glénan Archipelago	Granite with muscovite and biotite

Table 2 Geological description of the mentioned insular complexes

		Port Blanc	Standard deviation	Douet 23	Standard deviation	Douet 32	Standard deviationv	Belle-Ile	Ecart type	Granite Hoedic	Standard deviation
Na_2O	%	0,42	0,18	0,66	0,2	0,89	0,11	0,8	0,17	5,55	9,03
MgO	%	2,72	2,07	3,43	0,48	3,09	0,24	2,68	0,3	4,23	1,62
Al_2O_3	%	50,53	7,23	46,41	3,21	45,38	1,31	48,31	2,5	45,35	6,29
SiO_2	%	38,35	3,89	39,43	2,62	39,1	0,74	37,9	1,56	35,42	9,99
K_2O	%	1,87	0,35	1,5	0,41	1,83	0,32	1,54	0,19	1,11	0,53
TiO_2	%	0,98	0,63	1,34	0,5	1,47	0,21	1,1	0,22	1,01	0,63
MnO	%	0,07	0,05	0,1	0,06	0,1	0,05	0,09	0,03	0,06	0,05
Fe_2O_3	%	5,07	4,11	7,13	0,91	8,13	0,85	7,58	1,05	4,79	2,08
Li	ppm	560	503,9	406	208,35	351	90,69	1476	482,39	627	283,29
V	ppm	126	62,36	215	122,86	163	50,6	71	28,27	302	110,14
Co	ppm	23	19,68	38	15,2	34	6,05	45	19,22	43	19,6
Ni	ppm	30	15,65	47	12,98	48	5,54	45	13,93	29	29,54
Cu	ppm	3	0,33	9	7,11	4	1,64	1304	1771,55	53	38,32
Zn	ppm	257	247,17	425	188,54	371	140,9	621	237,41	502	232,59
As	ppm	1	1,23	4	2,88	2	1,37	38	56,35	21	14,14
Rb	ppm	664	450,74	911	398,01	700	229,05	1019	316,43	677	490,46
Sr	ppm	158	63,62	323	227,33	189	95,51	366	307,15	1039	1741,94
Y	ppm	6	12,36	76	98,51	12	7,57	21	19,54	41	53,85
Zr	ppm	34	45,57	1089	2375,9	26	16,9	430	594,9	1963	3298,49
Nb	ppm	60	42,19	73	35,94	84	28,08	91	25,4	56	33
Sb	ppm	0	0,03	0	0,1	0	0,32	1	0,71	1	1,6
Ba	ppm	403	127,13	952	1389,3	704	669,25	333	203,26	450	312,65
La	ppm	2	2,29	400	550,92	17	15,99	30	28,1	118	205,31
Ce	ppm	6	8,36	1191	1754,14	58	49,22	62	54,28	177	350,1
Pr	ppm	1	1,05	93	133,14	7	5,72	7	6,94	20	37,93
Nd	ppm	4	6,82	388	526,41	17	14,35	25	20,66	101	183,95
Sm	ppm	1	1,13	66	93,51	4	2,94	4	3,22	21	33,1

Eu	ppm	0	0,24	3	2,31	1	0,85	1	0,89	3	4,34
Gd	ppm	1	1,28	41	59,89	5	4,56	3	2,84	18	25,04
Tb	ppm	0	0,32	6	7,95	1	0,54	1	0,72	2	2,42
Dy	ppm	1	1,41	24	26,25	3	2,32	4	3,12	9	9,87
Ho	ppm	0	0,12	3	2,26	0	0,35	1	0,45	1	1,67
Er	ppm	0	0,83	6	5,06	1	1,12	2	1,33	5	5,65
Tm	ppm	0	0,08	1	0,47	0	0,11	0	0,16	1	0,79
Yb	ppm	0	0,41	3	1,95	1	0,44	1	0,95	3	4,79
Lu	ppm	0	0,11	1	0,44	0	0,1	0	0,14	1	0,93
Hf	ppm	1	1,31	38	64,17	2	2,81	10	9,41	33	48,42
Ta	ppm	7	6,59	8	3,75	8	3,8	14	4,16	6	3,34
Tl	ppm	5	3,38	5	2,1	5	1,5	8	2,6	5	3,98
Pb	ppm	9	7,98	33	26,45	16	3,62	2205	5499,82	70	29,58
Th	ppm	1	0,81	167	289,05	11	18,13	9	6,23	18	27,17
U	ppm	1	1,75	35	52,41	2	1,88	12	9,06	12	12,1

Table 3 Average chemical composition and standard deviation of biotite in potteries and granite from Hoedic and Belle-Île-en-Mer

		Ile aux Moutons Neo 4	Standard deviation	Ile aux Moutons Neo 3	Standard deviation	Ile aux Moutons Neo 9	Standard deviation	Ile aux Moutons Iron age 2	Standard deviation	Ile aux Moutons Iron age 4	Standard deviation	Ile aux Moutons Iron age 17	Standard deviation	Saint Nicolas 3	Standard deviation	Saint Nicolas 10	Standard deviation	Granite Ile aux Moutons	Standard deviation	Granite Archipel des Glénan	Standard deviation	Granite contiental (Beg Meil)	Standard deviation	Granite contiental (Trégunc)	Standard deviation
Na_2O	%	1,6	0,81	0,28	0,26	0,48	0,17	2,37	2,8	0,3	0,09	2,48	1,63	1,2	0,66	0,61	0,48	0,16	0,10	0,37	0,11	0,20	0,09	0,11	0,08
MgO	%	3,35	1,1	2,39	1,04	3,15	1,17	1,11	1,47	4,21	0,61	2,84	1,07	3,21	1,69	0,96	0,44	5,77	0,66	1,47	0,19	5,69	0,60	5,51	0,20
Al_2O_3	%	44,63	5,31	44,86	3,41	42,74	2,69	48,96	8,47	39,48	2	46,52	5,07	47,3	8,63	27,77	12,56	19,38	1,63	23,38	1,60	19,07	0,86	19,11	0,95
SiO_2	%	41,58	5,67	36,52	3,67	42,84	2,73	42,27	5,02	40,55	3,94	37,9	2,9	39,99	5,81	31,47	7,43	44,16	2,57	42,47	4,94	44,18	1,59	42,06	0,85
K_2O	%	1,15	0,21	1,83	0,87	1,48	0,5	1,3	0,72	1,74	1,1	1,38	0,58	1,41	0,68	1,6	0,8	3,71	0,76	1,96	0,84	4,11	0,21	3,50	0,80
TiO_2	%	0,06	0,02	1,24	0,42	1,36	0,37	0,45	0,51	1,26	0,77	1,03	0,49	0,88	0,56	9	17,68	1,65	0,46	1,09	0,41	1,27	0,14	1,83	0,21
MnO	%	6,49	1,75	0,07	0,03	0,09	0,07	0,06	0,08	0,06	0,01	0,04	0,02	0,12	0,08	0,41	0,77	0,25	0,06	0,69	0,15	0,20	0,05	0,47	0,04
Fe_2O_3	%	645,8	286,1	12,26	2,16	7,86	2,38	3,49	3,1	12,4	5,26	7,81	1,62	5,9	2,64	13,15	4,89	24,72	2,85	28,51	4,35	25,25	1,68	27,34	0,98
Li	ppm	646	286,02	1409	1196,59	179	65	131	103,76	58	24,86	85	47,91	596	419,52	1568	1564,14	743	267,65	6144	1995,01	128	26,37	975	151,74
V	ppm	214	62,43	217	187,43	222	88,53	73	37,72	488	219,23	243	100,99	202	121,29	492	325,7	299	106,72	50	15,08	488	101,56	319	68,54
Co	ppm	16	4,39	16	2,73	10	3,06	5	4,11	16	6,58	17	5,86	21	12,47	77	39,35	43	13,29	17	4,60	60	12,59	48	7,64
Ni	ppm	37	15,06	29	13,98	35	22,51	11	14,91	44	9,19	27	14,57	44	29,33	59	30,91	45	14,14	24	7,19	130	25,81	45	7,63
Cu	ppm	75	23,75	49	15,49	44	14,85	21	13,01	72	38,55	40	14,61	54	21,55	272	180,13	17	16,19	14	9,13	54	27,35	8	7,86
Zn	ppm	8	3,57	98	58,93	53	23,74	48	24,04	40	34,98	4	2,03	49	65,88	9	3,89	397	128,38	527	149,41	199	33,46	564	76,81
As	ppm	285	128,52	927	547,62	148	97,15	109	134,47	215	97,4	73	72,75	413	285,73	1597	2523,75	8	7,71	31	11,10	10	12,08	6	5,09
Rb	ppm	6	4,82	27	20,2	29	16,58	6	4,83	39	48,91	13	3,28	6	3,97	31	24,91	527	193,60	418	209,32	291	51,18	1146	799,43
Sr	ppm	609	168,89	845	542,19	400	281,49	287	269,02	357	242,33	252	154,32	709	514,74	954	1320,08	99	65,52	65	16,18	22	8,59	21	11,33
Y	ppm	139	94,79	179	126,58	227	204,37	513	819,65	88	62,95	368	484,84	428	263,06	3125	3611,85	10	11,69	24	25,57	37	113,81	37	48,04
Zr	ppm	21	28,78	6	4,43	16	7,07	5	0,91	36	48,57	21	10,79	52	97,89	186	181,71	174	445,94	183	361,12	210	611,84	79	269,92
Nb	ppm	322	247,22	109	94,46	225	397,29	157	166,88	51	28,37	98	50,11	1264	2888,86	840	1101,5	66	23,20	218	142,51	59	12,94	118	27,58
Sb	ppm	56	20,11	104	51,62	30	12,87	32	39,74	33	20,75	32	16,88	72	48,63	243	276,61	0	0,15	1	0,32	0	0,10	0	0,10
Ba	ppm	0	0,18	1	0,26	1	0,46	0	0,06	1	0,42	0	0,04	0	0,08	0	0,17	430	275,23	167	223,70	1163	247,07	694	816,35
La	ppm	294	173,27	240	139,32	301	101,55	169	59,2	295	225	155	45,08	856	815,45	666	537,74	196	589,59	216	613,78	611	1010,96	547	1208,48
Ce	ppm	11	9,86	16	19,69	29	11,36	19	20,99	72	102,69	40	24,65	50	77,49	148	138,7	127	335,39	166	514,72	302	525,85	352	799,46
Pr	ppm	21	18,83	29	34,37	57	22,2	29	28,08	147	214,93	104	85,14	109	140,78	497	539,11	68	148,44	91	244,18	159	255,39	216	387,07
Nd	ppm	2	1,79	4	4,35	8	3,31	5	2,67	24	35,77	9	5,58	11	14,24	60	67,45	59	125,93	64	160,79	123	200,56	170	275,61

Sm	ppm	13	12,97	13	15,69	32	14,5	12	8,65	104	154,73	37	22,22	54	82,21	246	300,9	34	70,98	45	106,49	70	107,59	90	136,83
Eu	ppm	2	1,95	5	7,05	6	3,03	3	1,58	19	28,5	6	3,42	9	10,7	87	98,69	7	5,62	21	34,67	38	54,75	31	34,47
Gd	ppm	1	0,26	0	0,37	1	0,6	0	0,26	4	5,03	2	1,06	2	2,88	4	3,86	22	44,68	30	53,28	43	69,27	60	77,58
Tb	ppm	2	3,77	2	1,41	5	2,17	2	0,85	12	18,07	4	2,51	9	9,33	65	78,38	18	35,12	27	37,22	41	55,04	44	58,57
Dy	ppm	0	0,72	0	0,37	1	0,31	0	0,06	2	2,63	1	0,45	2	2,59	7	7,74	13	23,81	20	24,04	31	49,73	34	48,20
Ho	ppm	5	8,68	2	1,73	4	1,7	1	0,51	10	14,14	4	1,75	12	17,13	36	42,82	10	17,63	15	17,37	26	44,26	25	35,42
Er	ppm	0	0,49	0	0,29	1	0,28	0	0,03	1	1,76	1	0,2	2	3,22	5	7,18	7	11,17	12	15,27	21	33,90	21	31,09
Tm	ppm	1	0,86	1	0,64	1	0,42	0	0,09	3	4,04	2	0,93	7	11,69	17	22,17	6	9,20	12	16,58	29	75,96	26	35,39
Yb	ppm	0	0,21	0	0,11	0	0,08	0	0,04	0	0,66	0	0,06	1	2,03	2	2,26	7	9,83	15	20,66	18	28,99	19	30,08
Lu	ppm	1	1,06	0	0,58	1	0,51	0	0,16	3	3,85	1	0,59	7	15,11	21	28,57	6	9,95	14	21,83	18	37,85	16	25,45
Hf	ppm	0	0,2	0	0,13	0	0,1	0	0,05	0	0,44	0	0,09	2	3,49	3	3,9	16	25,38	29	44,70	33	88,64	23	40,59
Ta	ppm	7	4,59	4	2,43	3	2,5	3	2,39	1	0,74	4	2,69	44	99,58	115	230,22	1	0,50	15	15,69	1	0,26	2	1,01
Tl	ppm	6	1,74	22	17,68	3	0,96	5	5,58	3	2,07	3	1,92	10	7,89	27	25,01	6	1,77	7	3,29	3	0,49	11	4,27
Pb	ppm	4	0,81	8	5,27	3	1,65	2	2,28	3	1,8	2	0,82	5	3,87	6	8,1	11	5,40	38	16,85	8	2,94	32	17,61
Th	ppm	16	4,11	29	26,46	52	29,75	27	2,34	54	53,8	40	38,22	22	13,16	42	27,36	56	150,29	105	349,23	91	294,49	68	141,29
U	ppm	5	4,48	27	41,66	25	13,39	14	6,04	75	43,5	48	21,15	26	28,68	229	281,92	4	5,38	117	329,00	5	11,18	113	395,19

Table 4 Average chemical composition and standard deviation of biotite in potteries and granites from the Glénan